ELSEVIER

Journal of Applied Geophysics 51 (2002) 11–20

JOURNAL OF APPLIED GEOPHYSICS

www.elsevier.com/locate/jappgeo

The importance of displacement currents in RMT measurements in high resistivity environments

Lena Persson [a,b], Laust B. Pedersen [a,*]

[a] *Department of Earth Sciences, Uppsala University, Villavägen 16, 752 36 Uppsala, Sweden*
[b] *Geological Survey of Sweden, Villavägen 18, 752 36 Uppsala, Sweden*

Received 5 October 2001; accepted 17 June 2002

Abstract

The effect of displacement currents on radiomagnetotelluric (RMT) measurements was analysed. It is shown that under normal crystalline bedrock conditions, displacement currents must be taken into consideration when modelling the RMT data. This is illustrated by the 1D inversion of the synthetic data, both for a homogeneous half-space as well as a layered earth. Finally, we show that the 1D inversion of the field data from Northern Sweden give more realistic, less conductive models of the sedimentary cover, when displacement currents are taken into account.

Keywords: RMT; Electric permittivity; Displacement currents; Crystalline bedrock

1. Introduction

It is a common assumption in applied electromagnetic geophysics that displacement currents can be neglected (see, e.g. Ward and Hohmann, 1988), and most modelling programs do not include them. However, in the standard radiomagnetotelluric (RMT), application frequencies ranging from 12 up to 250 kHz are used (Persson, 2001; Turberg and Persson, 1997). In areas with crystalline bedrock, the less fractured parts often have resistivities of up to 20 000 Ω m or even higher, and displacement currents may play an equally important role as the conduction currents. At still higher frequencies, they may even be used to characterise in detail the upper few meters of the subsurface, both with regard to conductivity as well as permittivity (Stewart et al., 1994). In this paper, a careful analysis of the influence of the dielectric effect is made.

2. The homogeneous half-space

The variation of the apparent resistivity ρ_a and phase ϕ for a homogeneous half-space with displace-

* Corresponding author. Department of Geophysics, University of Uppsala, P.O. Box 556, S-75122 Uppsala, Sweden. Fax: +46-18-501110.
E-mail address: lbp@geofys.uu.se (L.B. Pedersen).

0926-9851/02/$ - see front matter
PII: S0926-9851(02)00198-2

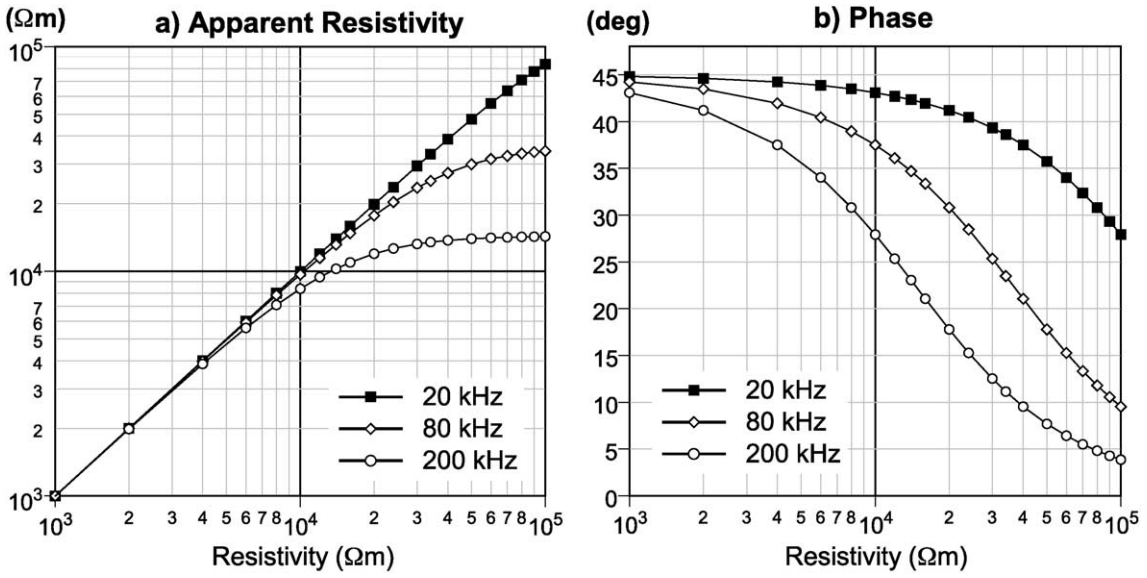

Fig. 1. Calculated apparent resistivity (a) and phase (b) as a function of the resistivity for the homogeneous ground. The relative electric permittivity, ε_r, is set to 5.

ment currents included was given by Crossley (1981). Taking the radio transmitters to be vertical electric dipoles, the dominant mode for distant radio transmitters will be that of the parallel incidence. The electric field in the air is predominantly vertical, while the magnetic field is predominantly horizontal. For a

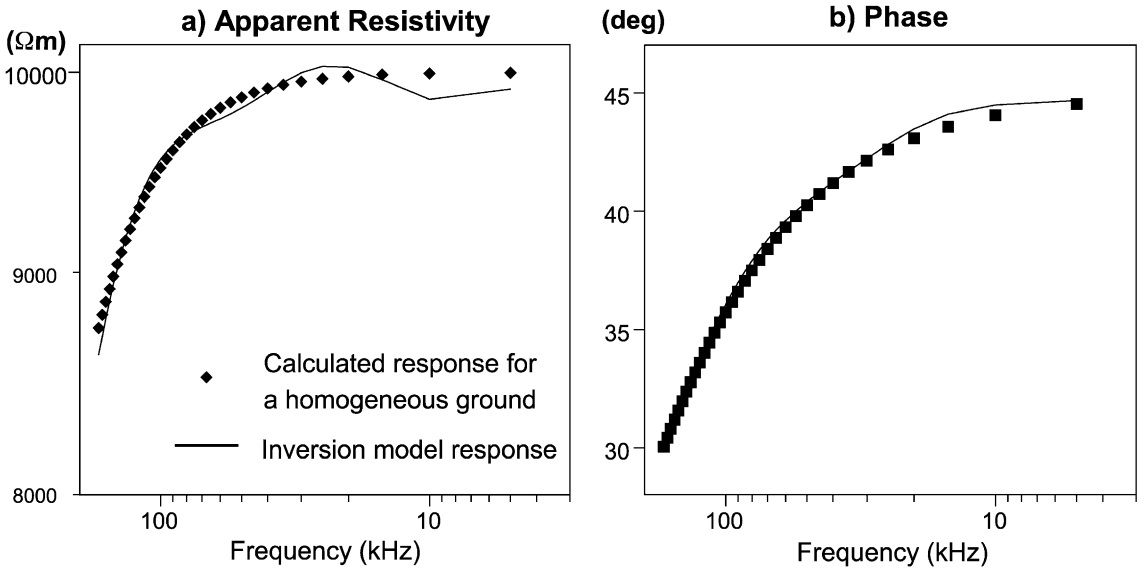

Fig. 2. Comparison between the original data from the homogeneous half-space (dotted lines) and predicted data (solid lines) from the 1D model shown in Fig. 3. During the 1D inversion, the displacement currents are neglected.

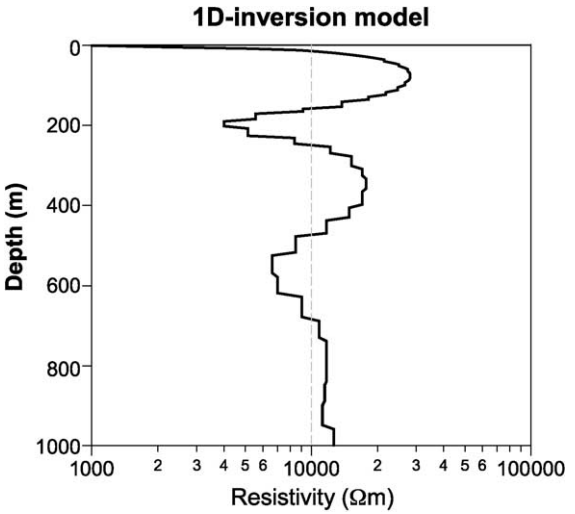

Fig. 3. 1D inversion model for a homogeneous half-space of 10 000 Ω m. Displacement currents are neglected during the inversion.

homogeneous half-space of resistivity ρ, permittivity $\varepsilon = \varepsilon_r \varepsilon_0$, and permeability μ_0, we have

$$\rho_a = \frac{\rho}{1+p^2}\left(1+p^2\left(1-\frac{1}{\varepsilon_r}\right)^2\right)^{1/2} \quad (1)$$

and

$$\phi = \tan^{-1} \times \left[\frac{\left(1+p^2\left(1-\frac{1}{\varepsilon_r}\right)^2\right)^{1/2} - p\frac{1}{\varepsilon_r}}{1+p\left(\left(1+p^2\left(1-\frac{1}{\varepsilon_r}\right)^2\right)^{1/2} + p\left(1-\frac{1}{\varepsilon_r}\right)\right)}\right] \quad (2)$$

where

$$p = \frac{\omega\varepsilon_0\varepsilon_r}{\sigma} = \omega\varepsilon_0\varepsilon_r\rho$$

and

ε_r = the relative electric permittivity.

The apparent resistivity ρ_a and phase ϕ were calculated from Eqs. (1) and (2) as a function of the resistivity for the three different frequencies. The result is shown in Fig. 1. In the calculations, we set $\varepsilon_r = 5$, which is typical for the crystalline rock like granite (see, e.g. Schön, 1995). Fig. 1a shows that the effect on the resistivity is negligible at 20 kHz.

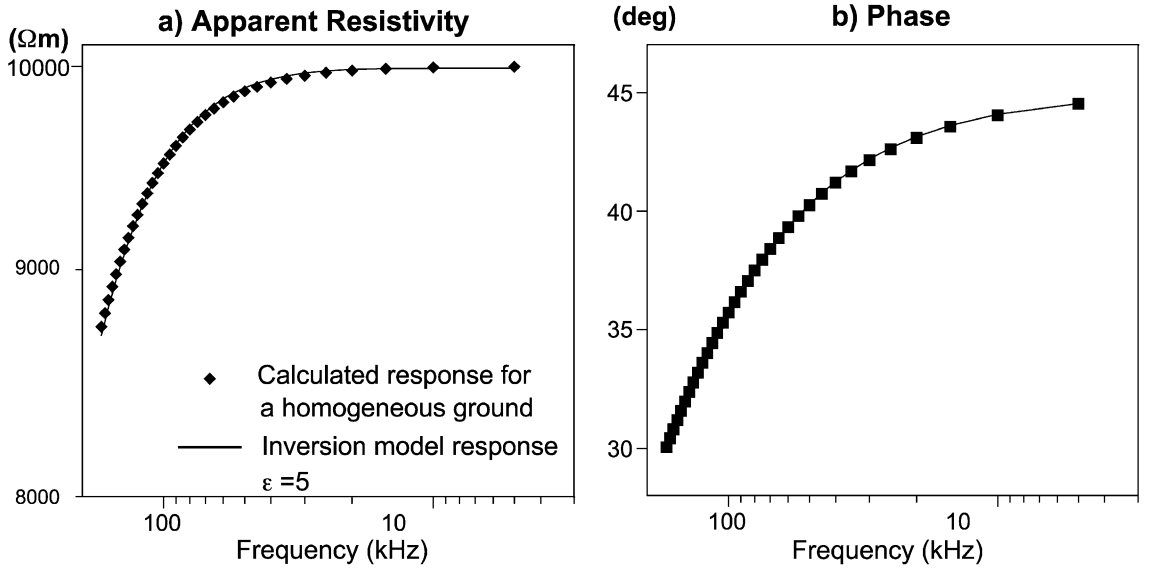

Fig. 4. Comparison between the original data from the homogeneous half-space (dotted lines) and predicted data (solid lines) from the 1D model shown in Fig. 5. During the 1D inversion, the relative electric permittivity is set to 5.

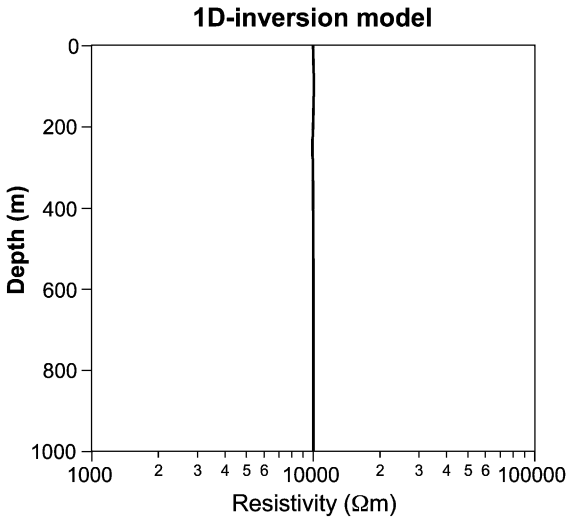

Fig. 5. 1D inversion model for a homogeneous half-space of 10 000 Ω m. The relative electric permittivity, ε_r, is set to 5.

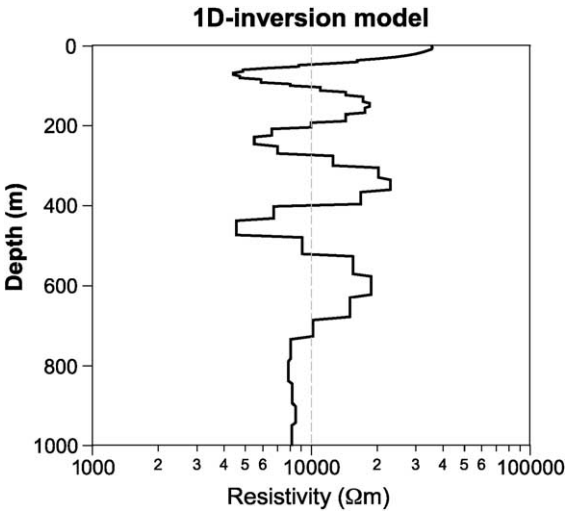

Fig. 7. 1D inversion model for a homogeneous half-space of 10 000 Ω m. The relative electric permittivity, ε_r, is set to 10.

However, at higher frequencies, the decrease in ρ_a becomes significant. For a homogeneous ground of 30 000 Ω m, the relative decrease in resistivity is 20% for 80 kHz and almost 50% for 200 kHz. The effect on the phase (Fig. 1b) is even more striking. Already at 20 kHz, the phase was reduced from 45°

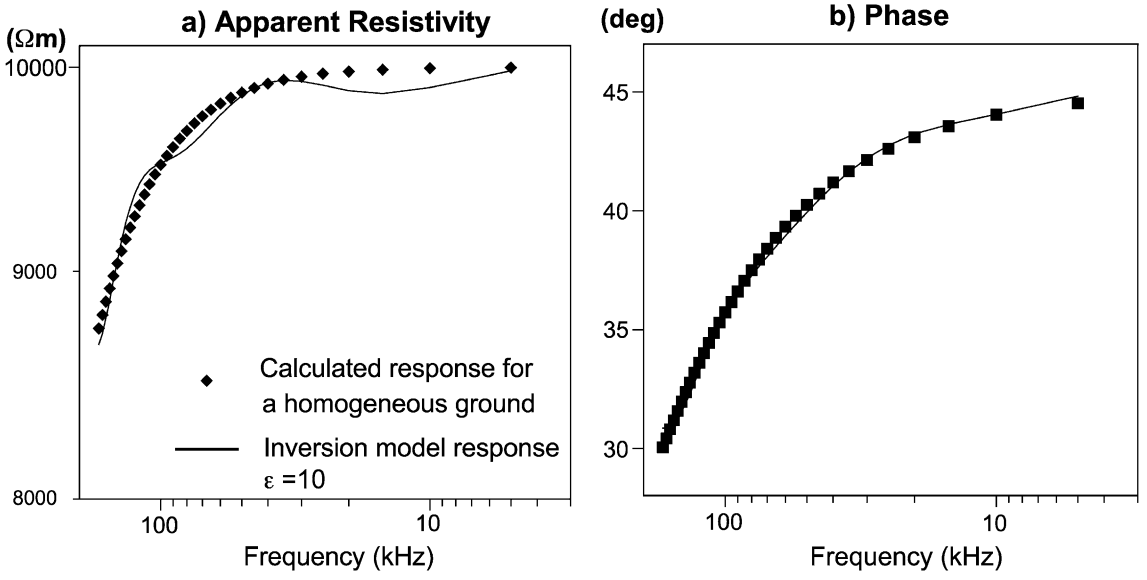

Fig. 6. Comparison between the original data from the homogeneous half-space (dots) and predicted data (solid lines) from the 1D model shown in Fig. 5. During the 1D inversion, the relative electric permittivity is set to 10.

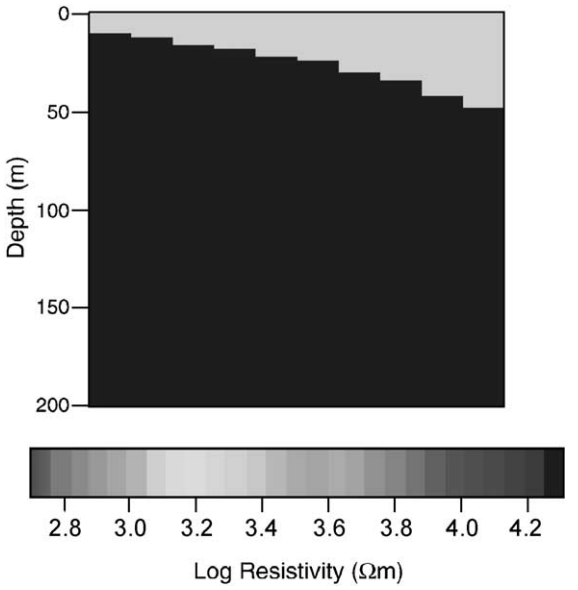

Fig. 8. Two-layered model with increasing depth of overburden. The resistivity of the overburden is 2000 Ω m while that of the host rock is 20000 Ω m.

to 40° for a homogenous ground of 30000 Ω m, for 80 kHz, the phase was reduced to 25° and for 200 kHz, the phase becomes as low as 12°.

3. Synthetic models

3.1. Homogeneous half-space

The result shown above indicates that the effects of displacement currents cannot be ignored for LF-frequencies (30–300 kHz), especially over a resistive ground. Another way to study this effect is to ignore it when inverting the data and see what distortion, away from the true model, it gives rise to.

The response for a homogeneous half-space with a resistivity of 10000 Ω m was calculated, using Eqs. (1) and (2), for frequencies ranging from 1000 up to 170000 Hz. Also, here we set the relative electric permittivity $\varepsilon_r = 5$. The data were then inverted without taking the displacement currents into account using the truncated singular value

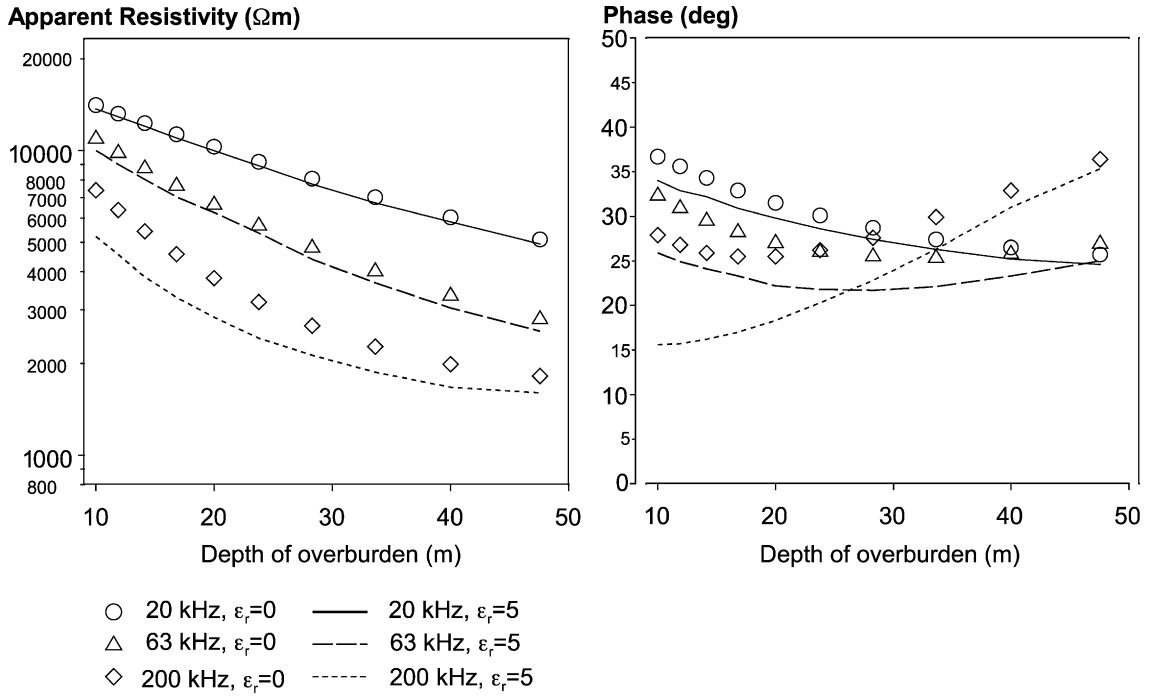

Fig. 9. Calculated 1D response (apparent resistivity and phase) for the model in Fig. 8 both with and without considering the effect from the displacement currents. The case $\varepsilon_r = 0$ corresponds to neglecting the displacement currents.

decomposition approach by Pedersen (submitted for publication). Fig. 2 shows the data response for the apparent resistivity and phase, and Fig. 3 shows the inverted model. No perfect fit was achieved between the data response from the 10 000 Ω m half-space and response from the inverted model. In particular, for the apparent resistivity data, there was no possibility to find a model that completely explains the data response. However, taking into account that real data may have errors of say 2% on the apparent resistivity and 1/2° in phase, the fit is satisfactory.

The inverted model (Fig. 3) shows a low resistive layer at the top followed by alternating layers of high and low resistivity. The top layer has a resistivity of 1000 Ω m, which is one tenth of the true model of 10 000 Ω m. For a homogeneous half-space model, the conclusion is that neglecting displacement currents during the inversion will cause a distorted model with a conductive layer on the top followed by a very highly resistive layer.

The 1D inversion code was then modified to take into account the effect of displacement currents. The relative electric permittivity ε_r was fixed to 5 during the inversion. Figs. 4 and 5 show the inversion result and inverted model, respectively. We see that now a perfect fit is achieved and the true model (homogeneous half-space) is found.

If a wrong value for the relative electric permittivity is used during the inversion, we will again get a distorted model. In Figs. 6 and 7, the relative electric permittivity is set to 10. In this case, we see that there is no possibility to find a model that explains the data response completely. In contrast to Fig. 3, we now get a model with a high resistivity at the top followed by a very low resistivity.

3.2. Layered earth models

The next example shows the results from a more realistic model with a resistive bedrock covered by a conductive overburden. The resistivity of the overburden and bedrock are 2000 and 20 000 Ω m, respectively. The depth of the overburden varies from 10 down to 45 m as shown in Fig. 8. To

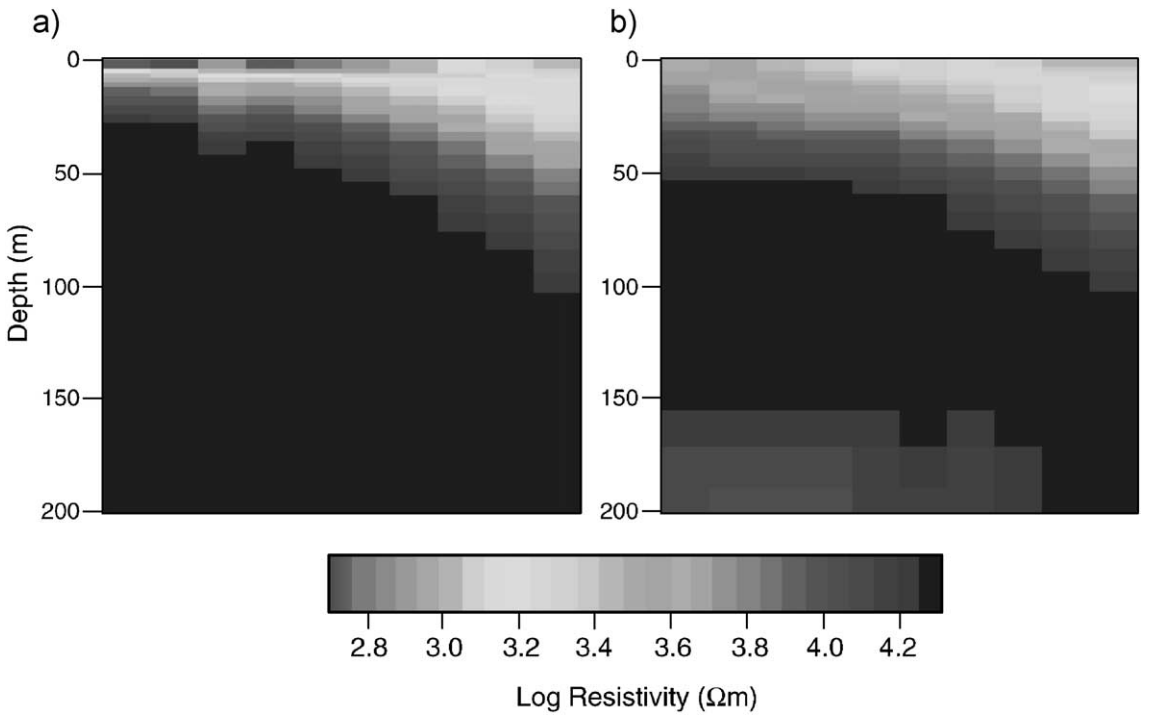

Fig. 10. Stitched 1D inverted models when ignoring displacement currents (a) and when the electric permittivity, ε_r, is set to 5 (b).

resemble the field measurements, only three frequencies are used for the forward calculations: 20, 63 and 200 kHz, respectively. Fig. 9 shows the calculated 1D response for the model, both with and without considering the effect from displacement currents. As expected, the effect is largest for the highest frequency as well as for the small thickness of the overburden, where the apparent resistivity becomes large.

The response for $\varepsilon_r = 5$ (solid lines in Fig. 9) was then inverted with the 1D code used in the above examples. Fig. 10a shows the inverted 1D model neglecting the effect of displacement currents. We see that the upper part of the inversion model has a much lower resistivity than the true model (approximately 500 Ω m as compared to 2000 Ω m). In the model, resistivities higher than 20 000 Ω m have been suppressed in order to enhance the resolution in the upper layers, but the bedrock part of the model shows resistivities that are considerably higher than 20 000 Ω m.

Fig. 10b shows the inverted model from the modified 1D code, where the effects of displacement currents are taken into consideration. As expected,

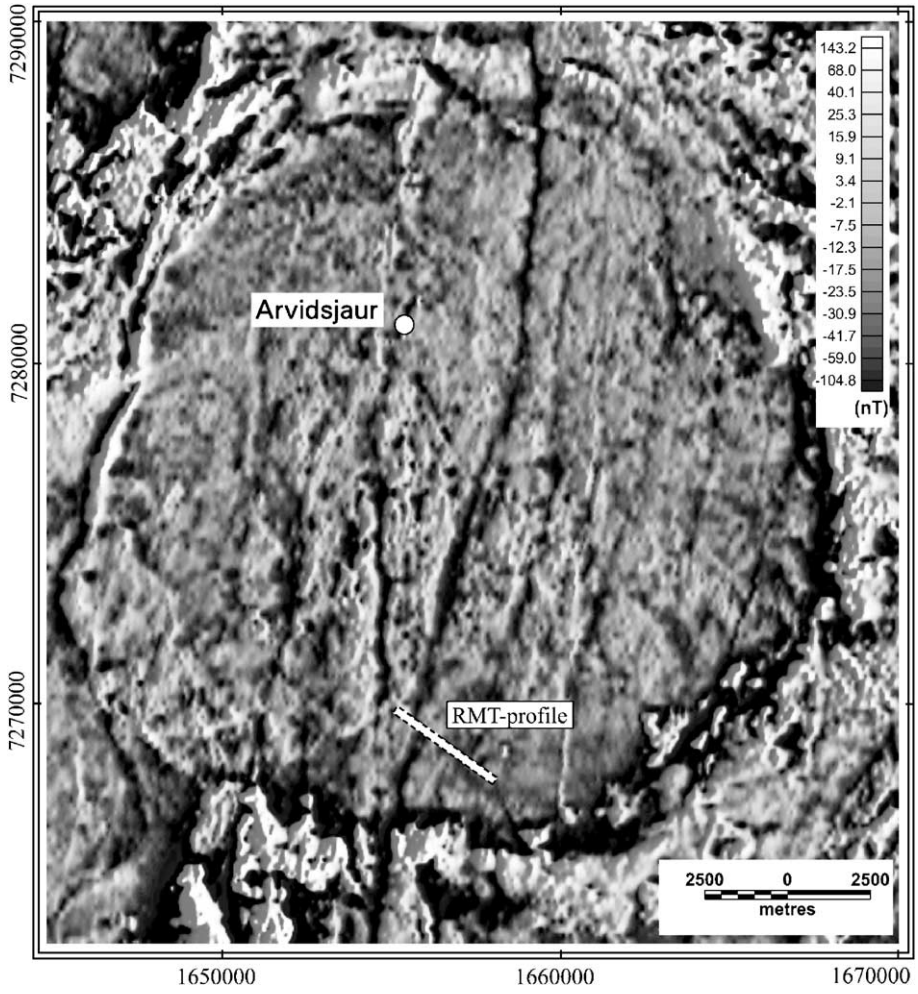

Fig. 11. Airborne magnetic map (residual field) over the Arvidsjaur granite intrusion (data source: Geological Survey of Sweden). The location of the RMT profile is shown by a white line.

this model shows more similarity with the true model. Despite the smooth images obtained, the estimated resistivities of the overburden and host rock lie close to the true values of 2000 and 20 000 Ω m, respectively.

4. Application to field data

During the 2D inversion of some real RMT profile data, it was observed that along some parts of the profiles very low phases were measured that were

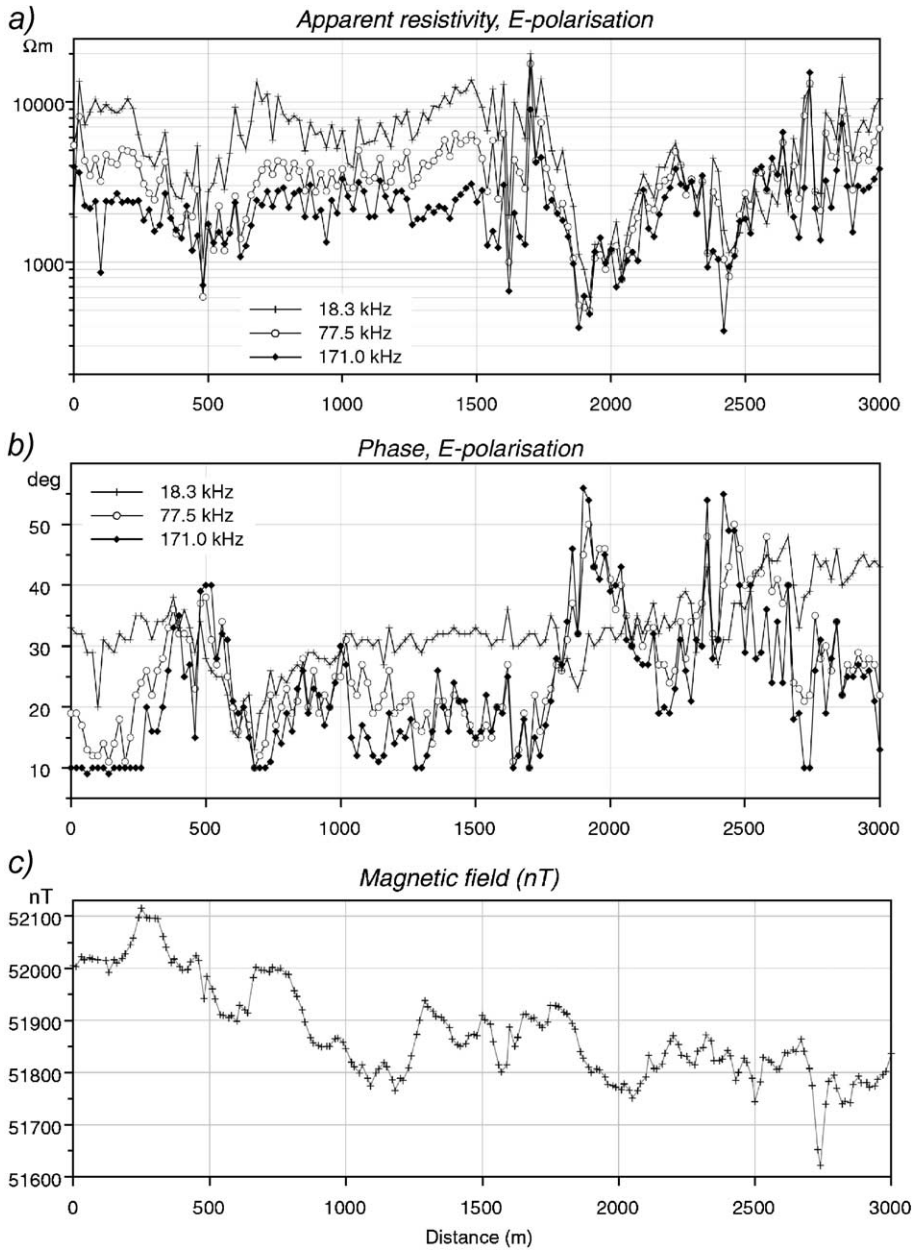

Fig. 12. Apparent resistivity (a), phase (b) and total magnetic field (c) along the RMT profile.

impossible to fit with the 2D model. This phenomenon is observed for the higher frequencies and on a resistive ground. A possible explanation is that the measured response is influenced by the dielectric effect. In the available 2D inversion codes, there is no possibility to take the effect of displacement currents into consideration during the inversion. However, the effect will only be significant on the resistive ground outside the fracture zones and other conductive structures.

Fig. 11 shows the airborne magnetic map over the Arvidsjaur granite intrusion in Northern Sweden. The location of a 3-km-long RMT profile is also shown on the map. Fig. 12 shows the measured data (resistivity and phase together with the total magnetic field) from the RMT profile. A 400-m-long part of this profile (coordinates 1000–1400 m in Fig. 12) is selected to illustrate the effect of displacement currents on the field data. This section represents a fairly homogeneous part of the profile with no observable two-dimensional effects. E-polarisation mode data, i.e. currents running approximately parallel to strike, for three frequencies (18.3, 77.5 and 171.0 kHz) are used for the 1D inversion.

Fig. 13a shows the inverted 1D model when neglecting the displacement currents. Only the upper-

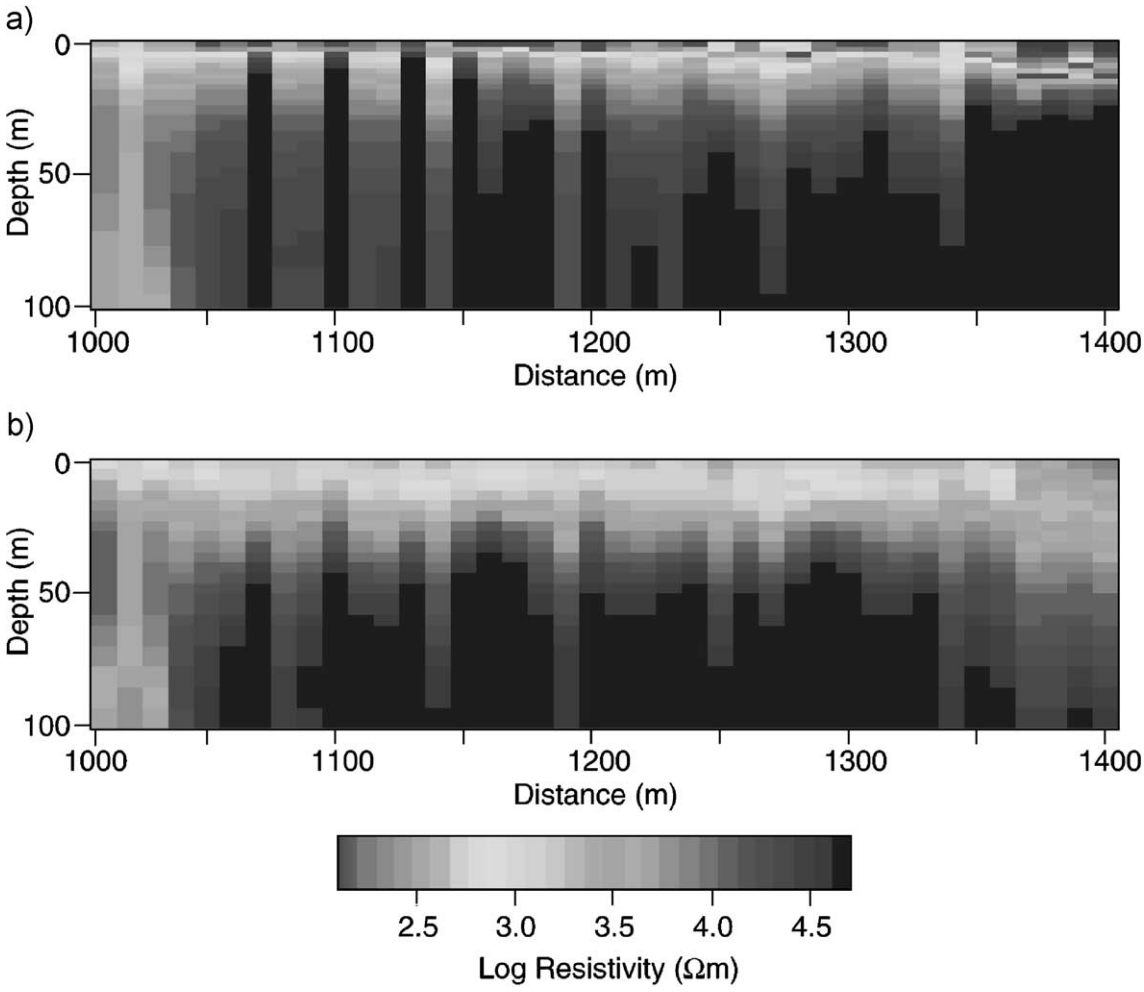

Fig. 13. 1D inverted model along 400-m part of the Arvidsjaur profile. In the upper model (a), the displacement currents are ignored during the inversion, while in the lower model (b), the displacement currents are taken into account and the relative electric permittivity, ε_r, is set to 5.

most 100 m of the model is shown. A thin conductive layer, corresponding to the overburden, is present at the top with resistivities of around 100 Ω m. No evidence of such a conductive layer was observed along this part of the profile. Moreover, the layer is somewhat inhomogeneous with varying depths along the profile.

In Fig. 13b, the inverted model from the modified 1D code, where the effect of displacement currents is taken into consideration, is shown. This is a more likely model with a low-resistivity layer of around 1000 Ω m, a resistivity that can be expected for a water-saturated moraine. The depth of the overburden is approximately 25 m, and the layer is much more homogeneous compared to the previous model. This result is also confirmed by two electrical soundings measured close to the RMT profile that gave a thickness on the overburden of around 25–30 m, with a resistivity of around 2000 Ω m.

5. Discussion and conclusions

The main conclusion of this paper is that the effect of displacement currents must be considered when modelling RMT data over resistive formations and rocks. Taking into account that phase errors of the measured impedances can easily be as small as half a degree, it means that even for resistivities less than 1000 Ω m, their effect will be well above the error level. Since the relative permittivities of rocks and loose sediments normally lie within the range of 4–10, it can be argued that fixing the relative permittivity to say 7 is a better alternative than neglecting it, i.e. setting it equal to zero.

We even made an attempt to invert the data for the unknown permittivity using the 1D models. Given that the permittivity varies only by a factor of 2, between 4 and 8, the maximum frequency is 250 kHz and that resistivities are less than 20 000 Ω m, we have not observed such differences in the resulting resistivity models that the extra calculations are justified.

The geophysical example from Northern Sweden clearly demonstrates that the unrealistically low resistivities obtained when neglecting displacement currents can be avoided by setting the relative permittivity to five. Furthermore, the thickness of the loose sediments thereby becomes much more realistic.

References

Crossley, D.J., 1981. The theory of EM surface wave impedance measurements. In: Collet, O.J., Jensen, O.G. (Eds.), Geophysical Applications of Surface Wave Impedance Measurements. Geol. Surv. Can., Pap., vol. 81-25, pp. 1–17.

Pedersen, L.B., 2002. Least singular value decomposition inversion of magnetotelluric data. Geophysical Prospecting submitted for publication.

Persson, L., 2001. Plane wave methods for imaging fracture zones. Acta Universatis Upsaliensis, Uppsala dissertations from the Faculty of Science and Technology 30. ISBN 91-554-5028-8.

Schön, J.H., 1995. Physical Properties of rocks: fundamentals and principles of petrophysics. In: Helbig, K., Treitel, S. (Eds.), Handbook of Geophysical Exploration, Section 1: Seismic Exploration. Pergamon, Oxford, UK, pp. 399–405.

Stewart, D.C., Anderson, W.L., Grover, T.P, Labson, V.F., 1994. Shallow subsurface mapping by electromagnetic sounding in the 300 kHz to 30 MHz range—model studies and prototype system assessment. Geophysics 59, 1201–1210.

Turberg, P., Persson, L., 1997. Radiomagnetotelluric measurements for detection of faults and fracture zones in Sweden. 59th EAGE Conference and Technical Exhibition Geneva, Switzerland, 26–30 May 1997. Extended abstract of papers, F-20.

Ward, S.H., Hohmann, G.W., 1988. Electromagnetic theory for geophysical applications. In: Nabighian, M.N. (Ed.), Electromagnetic Methods in Applied Geophysics, Theory. Soc. Explor. Geophys., vol. 1, pp. 131–311.